Int J Adv Manuf Technol (2010) 50:1–12
DOI 10.1007/s00170-009-2488-7

ORIGINAL ARTICLE

Development of a pad conditioning simulation module with a diamond dresser for CMP applications

Hsiu-Ming Yeh · Kuo-Shen Chen

Received: 12 August 2009 / Accepted: 14 December 2009 / Published online: 22 January 2010
© Springer-Verlag London Limited 2010

Abstract Chemical mechanical polishing (CMP) is a key fabrication route for the modern semiconductor process. The degradation of the polishing pad during the polishing process can significantly influence the polishing performance. Therefore, pads need to be conditioned frequently and an efficient emulator for the dressing process optimization is required to guide the dressing process. In this work, a pad condition simulation module is designed and demonstrated. In addition, a new performance index, called as recover–area ratio (RAR), is defined. Subsequently, a series of parametric studies are performed to investigate the influence of key geometric or processing parameters for a pad conditioning process in terms of optimizing the conditioning performance. Finally, results reveal that it is possible to correlate the pad RAR and Preston's constant variation and to integrate the pad conditioning emulator with the pre-developed CMP polishing simulation module as a whole utility to further optimize the existing CMP processes.

Keywords Chemical mechanical polishing (CMP) · Dressing · Computer simulation · CAD · Preston's constant

H.-M. Yeh · K.-S. Chen
Department of Mechanical Engineering,
National Cheng-Kung University,
Tainan, Taiwan 70101, Republic of China

K.-S. Chen (✉)
Center of Micro/Nano Science and Technology,
National Cheng-Kung University,
Tainan, Taiwan 70101, Republic of China
e-mail: kschen@mail.ncku.edu.tw

1 Introduction

The chemical mechanical polishing (CMP) process is a key fabrication route in state of the art integrated circuit (IC) fabrication processes [1]. The global uniformity of the material removal rate (MRR) is critical for short-wavelength optical lithography and copper fabrication processes, as well as for device yield considerations. The CMP process, schematically shown in Fig. 1, consists of a wafer carrier, a carrier film, and a pad attached to a rigid platen. When planarizing the wafer surface, the pad is placed on the platen with a uniform external applied load. A chemical slurry is sprayed continuously on the pad. Both the wafer and the pad rotate and their relative motion brings the wafer in contact with aggregates in the slurry, which generates multiple actions, including the mechanical shearing and chemical reaction, to remove the material. The detailed mechanism of the CMP process is quite complicated and not yet fully described due to the complexity of the interaction between the structural, chemical, fluid, and material domains. Phenomonologically, the MRR of the CMP process can be predicted by semi-empirical formulas such as the Preston equation [2], i.e.,

$$\mathrm{MRR}(\mu\mathrm{m/min}) = KPV, \tag{1}$$

where P is the interfacial pressure, V the relative velocity, and K a proportional constant, which is related to material prosperities, pad characteristics, slurry chemistry and aggregates, and even fluid dynamics [3, 4].

Polishing pads play a critical role in the CMP process and they are usually made of soft and porous polymeric materials containing numerous micro voids and tiny asperities for holding the aggregating particles and maintaining the fluid pressure for microscopic material removals [5–7]. Many previous researches focused on the effect of

SUNG EXHIBIT 2009
IPR2024-533

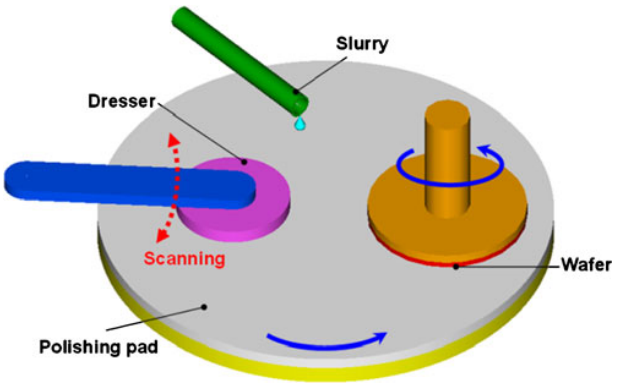

Fig. 1 Schematics of a CMP dresser system

contact stress distribution between wafer and pad on MRR. For example, see [8–11]. However, from microscopic viewpoint, during the polishing process, the debris generated continuously fills in the voids and this reduces the pad capability in terms of holding aggregates and slurries. As a result, the effective Preston's constant, as well as the MRR, both decrease. In order to recover the performance of pads, dressers that contain diamond grit arrays are usually employed. By periodically moving this dresser on a rotating pad, a thin surface layer of the pad can be removed to form a fresh interface and the performance of the pad can be recovered. From practical point of view, there are two major concerns for a dressing process: the dressing rate (pad cutting depth per unit of time) and the dressing uniformity. Most of the related studies on pad dressing are experimental investigations. For example, Liao et al. [12] investigated the effects of diamond spacing, diamond leveling, and substrate flatness on the influence of pad dressing rate. Zhou et al. [13] performed experiments to evaluate the influences of the conditioner's rotating speed, the conditioning load, and the conditioning time for MRR and the associated within-wafer nonuniformity for process optimization. On the other hand, the work performed by Sung et al. [14] indicated the strong correlation between the pad dressing rate and the wafer removal rate. Finally, Tsao et al. [15, 16] performed investigations to discuss the effect of pad aging, soaking time, the *pH* level of slurries, conditioning load, conditioning speed, and conditioning time. In addition, based on their experimental results, an empirical formula on the dressing rate was proposed as

$$\text{Dressing rate} = K_{\mathrm{D}} \frac{V_D}{RA} \lambda d_0 \left(\frac{P}{H_{\mathrm{p}}} \right)^{1.5}, \tag{2}$$

where K_{D} is the dressing coefficient; V_{D} the dressing speed; R and A are the effective radius and the cutting area of the dresser, d_0 and λ the effective radius and the distributed density of the diamond grits, and P the applied load. Finally, H_{p} is the pad hardness.

Meanwhile, the removal uniformity is also a major concern and it is a function of processing kinematic parameters such as rotating speeds, swing angles, and diamond patterns. Without careful planning, it may require a significant amount of time to finish a dressing process or one with a poor uniformity. In the worst scenario, the cutting path would even be synchronous and certain portions would never be dressed. As a result, how to determine the necessary parameter values to yield an efficient dressing is not a trivial issue. Hu [17] developed a simulation tool for diamond dressers to investigate the relationship between the cutting path and the surface topology generated according to various processing parameters such as dressing speed, size of dresser, and pattern and density of diamond grits. Tyan [18] analyzed the kinematics associated with the dresser-pad movement and proposed an index, called as the pad conditioning density (CD), as the measure of dressing performance, which is defined as the (time) average of total segment length per unit area in the radial direction (see Eq. (3.2) of ref [18]). It represents the ratio between the dressed area and the total pad area. In addition, he also performed studies to evaluate the effect of various processing parameters on the CD. However, from a practical perspective, a specific location of a pad which has been dressed does not mean that this area can be fully functional. That is, it may require several "cuttings" such that the glazed layer can be fully removed. The cutting depth, as well as the thickness of the glazed layer, is highly process-parameter-related information. As a result, the above definition should be modified to include the influence of other related information. In general, previous works usually emphasize the trajectory prediction. However, from a practical view point, the most important issue is how to remove the ineffective layer to recover the Preston's constant as soon as possible. As a result, one should use this issue to evaluate the dressing performance. Practically, it may be reasonable to assume that the local Preston constant recovery ratio is also a function of dressing depth. Once the glazed layer is removed, the Preston's constant can be fully recovered. In this work, we aim to propose a more generalized performance measure and to develop a dresser emulator to evaluate the effect of key dressing parameters on the dressing efficiency for CMP applications.

A new performance index, called as recover–area ratio (RAR), is defined as

$$\mathrm{RAR}(\%) = \frac{\sum A_{\mathrm{Ri}}}{A_{\mathrm{pad}}} \times 100\%, \tag{3}$$

where A_{pad} and A_{Ri} are the pad and the final recovered areas, respectively. Physically, RAR means the ratio between the recovered and total pad areas, which directly maps the engineering concern into the subsequent analysis. On the contrary, as mentioned above, the previous

SUNG EXHIBIT 2009
IPR2024-533

performance index, CD, is merely the ratio between dressed and the total pad areas, which cannot reflect the effectiveness of the dressing performance. That is, it might require multiple cuts for a specific portion before the glazed layer is finally removed. Using RAR as the performance measure, a dresser emulator is developed to predict the dressing efficiency and the recovery of the effective Preston's constant. Subsequently, we like to integrate this dresser module with our developed wafer level CMP CAD system.

The rest of this work presents the development and simulation of the CMP dressing in detail and is organized as follows. In Section 2, the kinematic analysis for modeling the trajectory of a dresser on the associated pad is explained. Based on the kinematic analysis, in Section 3, the simulation module is constructed and the necessary simulations and parametric analyses are performed in Section 4. Section 5 provides a brief discussion to highlight the important conclusions drawn from this work and possible future perspectives. Finally, Section 6 concludes this paper.

2 Kinematics analysis

The dressing model (i.e., Eq. 1) governs the instantaneous pad removal rate after the dresser passes over a specific portion of a pad. However, the global performance actually depends on the trajectory planning, which is influenced by the rotating speed of the dresser, the swing speed and range of the dresser arm, as well as the pad speed. In order to design a CMP dresser emulator, the relative speed between the dresser and the pad must first be analyzed. Schematically, the interaction between the diamond dresser and a pad is shown in Fig. 2. The parameters shown in Fig. 2 are listed below.

ω_s	Absolute angular velocity of the dresser
ω_p	Absolute angular velocity of the pad
θ_d	Swing angle of the dresser
l	Length of the dresser arm
r_{dp}	Position vector of the dresser center O_d relative to the center of pad O_p
r_d	Position vector of contact point p relative to the dresser rotational axis
r_c	Radius of the dresser
r_{pad}	Radius of the pad
(l_{cx}, l_{cy})	Position of the rotational axis of the dresser

In this work, it is assumed that the dresser is moved back and forth sinusoidally. As a result, the swing angle θ_d can be expressed as

$$\theta_d = \theta_s \times \sin \omega_s t, \tag{4}$$

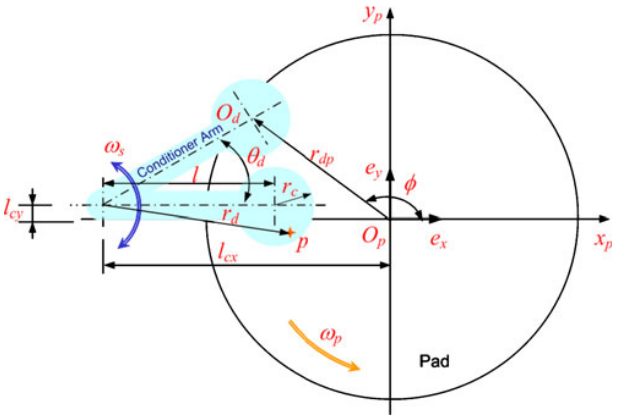

Fig. 2 The schematic of pad/dresser system and the definitions of necessary parameters

where θ_s is the maximum swing angle and t the time for conditioning. On the other hand, from geometry, the position vector of the dresser center $\overrightarrow{r_{dp}}$ can be expressed as

$$\overrightarrow{r_{dp}} = r_{dpx}\overrightarrow{e_x} + r_{dpy}\overrightarrow{e_y}, \tag{5}$$

where

$$\begin{aligned} r_{dpx} &= l_{cx} + l\sin(\theta_s \cdot \sin \omega_s t) \\ r_{dpy} &= l_{cy} + l\sin(\theta_s \cdot \sin \omega_s t). \end{aligned} \tag{6}$$

And the position angle ϕ shown in Fig. 2 is

$$\phi = \tan^{-1}\left(r_{dpy}/r_{dpx}\right). \tag{7}$$

In addition to the swing motion, the rotation of the pad must also be considered. By kinematics, the position of the dresser center relative to the rotating pad is expressed as

$$\begin{aligned} r_{px} &= r_{dp}\cos\left(\phi - \omega_p \cdot t\right) \\ r_{py} &= r_{dp}\sin\left(\phi - \omega_p \cdot t\right). \end{aligned} \tag{8}$$

By Eq. 8, it is possible to determine the path of the dresser center on the associated pad and the possible covering area by dresser radius, r_c. In addition, a dimensionless rotating speed ratio ω_R is defined as

$$\omega_R = \omega_s/\omega_p, \tag{9}$$

for the purpose of subsequent parametric studies discussed in subsequent sections.

3 Construction of the simulation module

By the results of kinematics modeling performed in Section 2, it is possible to integrate the kinematic analysis, material information, and necessary I/O under a CAD environment. The idea is straightforward. That is, in order to perform the analysis, the computational domain (i.e., the

SUNG EXHIBIT 2009
IPR2024-533

CMP pad) must be split into numerous cells. By using the kinematic analysis, it is possible to find the overlapping zone between the dresser and the pad at any time. For any specific moment, the pad removal rate can be calculated using Eq. 2. By utilizing the trajectory prediction and pad removal rate equation (i.e., Eq. 2), it is possible to calculate the pad removal of any cells and subsequently the dressing contour or dressing uniformity over the entire pad.

The algorithm for performing the above computation is shown in Fig. 3 and is briefly introduced below. At a given time, the coordinate of the center of the pad **rdp(i,j)** can be calculated. By individually checking the distance **cellr(i,j)** of all pad cells **rp(i,j)** with the dresser center, those pad cells to be dressed can be determined. By kinematics, both the velocities of the pad and the dresser at the same location can be determined simultaneously. The sliding velocity is then determined by simply performing a vector subtraction of those two quantities. Once the sliding velocity has been determined, it is possible to find the dressing depth at this time increment using Eq. 2. By continuing to the next time increment, the whole process can be repeated until the processing time is finished.

```
Algorithm: Pad dressing
for t=0:dt:T
   Vdp= ωp*rdp;          (find initial velocity of dresser center on the pad)
   for i=1:n
      for j=1:n
         cellr(i,j)=rp(i,j)-rdp(i,j);          (get cell position)
         if cellr(i,j)<=rc
            Vp(i,j)=ωp*rp(i,j);              (find velocity of individual cell on the pad)
            Vd(i,j)=ωs*rd(i,j);              (find velocity of individual cell on the dresser)
            Vds(i,j)=Vd(i,j)-Vp(i,j);        (calculate relative velocity)
            padZ(i,j)=padZ(i,j)-dz*Vds(i,j)/Vdp;    (find pad thickness of individual cell)
         end
      end
   end
end
```

The pad conditional module is written using MATLAB. As mentioned above, the computational domain is the entire polishing pad, which is mathematically separated into numerous rectangular cells. The simulation flow is shown in Fig. 3. By firstly specifying the necessary parameters from both the geometric and processing settings (listed in Table 1), as well as the computational setting, the module then calculates the amount of dressing at a given time increment by applying the algorithm shown in Fig. 3. The process is repeated again until the time step is finished. The results are then collected and visualized to reveal important information such as RAR and cutting profiles. Notice that the placement of the dresser also affects the conditioning results. Two typical dressing placements are shown in Fig. 4. It is convenient to distinguish between them using the azimuth angle θ_i (i.e., θ_i=90° for situation (a) and θ_i= 180° for situation (b)). In addition, the effects of different types of dresser swing angles are also investigated. As shown in Fig. 5, one is from 0 to θ_s. The other one is from $+\theta_s$ to $-\theta_s$. In this study, θ_s=40°, which is a typical setting

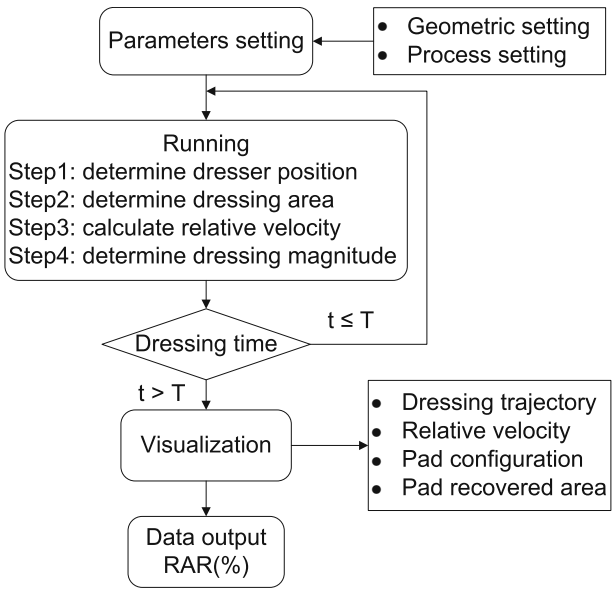

Fig. 3 Schematic of pad conditioning simulation module

SUNG EXHIBIT 2009
IPR2024-533

Table 1 Detail setting parameters of the pad conditioning simulation module

Geometric setting	Pad size, cellular size, dresser arm length, dresser initial position, and dresser disk size	
	Grooved pad parameters:	Grooved pitch, grooved depth, and grooved width
Process setting	Pad:	Angular velocity
	Dresser:	Angular velocity, swing angle, swing routes, dressing time
Visualization	Dressing trajectory, relative velocity, pad configuration, and pad recovered area	

for state of the art dressing systems. Notice that in the study presented by Tyan [18], the patterns of diamond grits have no significant influence on the final dressing results. As a result, in this work, we assume that the diamond grits are uniformly distributed on the dresser.

4 Simulation and parametric studies

This section presents the essential demonstration and parametric studies using the constructed process emulator.

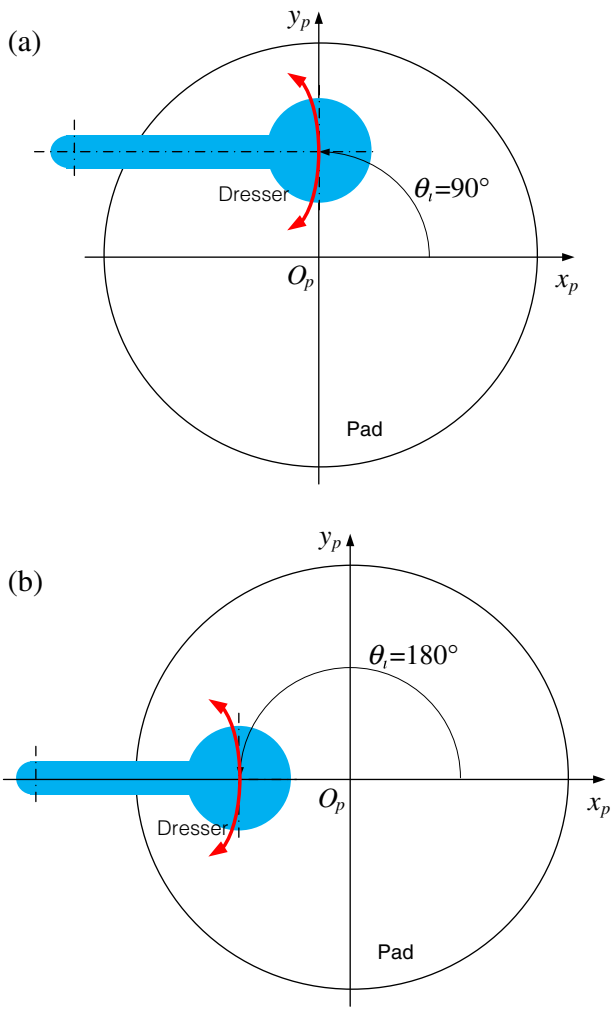

Fig. 4 Definitions of the dresser initial position, **a** θ_i=90°, **b** θ_i=180°

4.1 Trajectory demonstration

Figure 6 shows the trajectory of the dresser center on the pad for different dresser rotating speeds ranging from 10 to 60 rpm while the pad speed ω_p is fixed at 70 rpm with an arm length l=610 mm. The dressing period is 6 s with a θ_i of 90° and a swing angle of between 0 and 40°. The radius of the CMP pad is 390 mm. From Fig. 6, it can be seen that the trajectories generated are different, and this

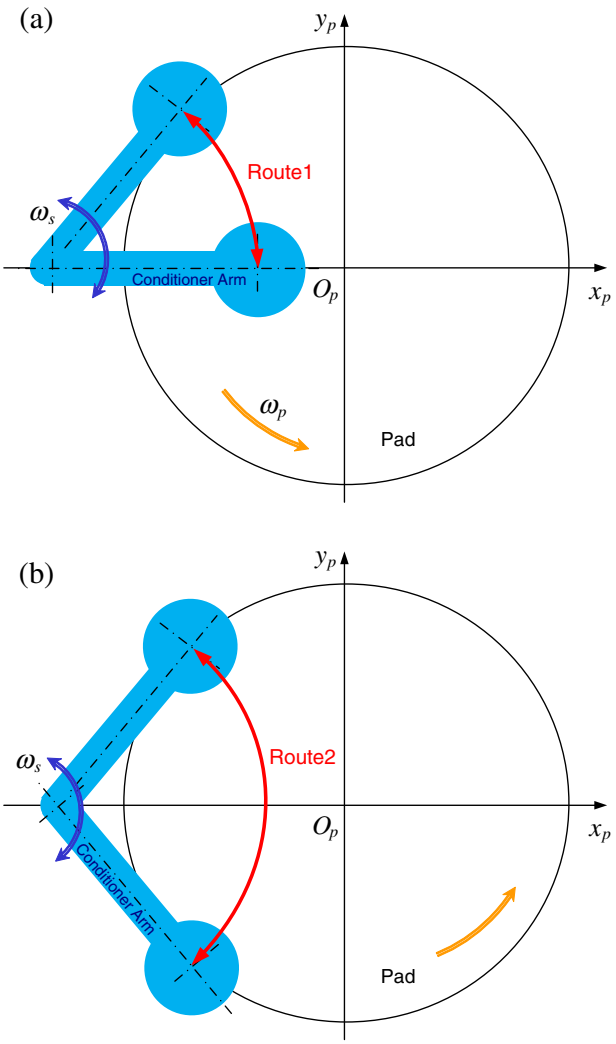

Fig. 5 Definitions of the dresser swing routes, **a** Route1=0~θ_s, **b** Route2=−θ_s~θ_s

SUNG EXHIBIT 2009
IPR2024-533

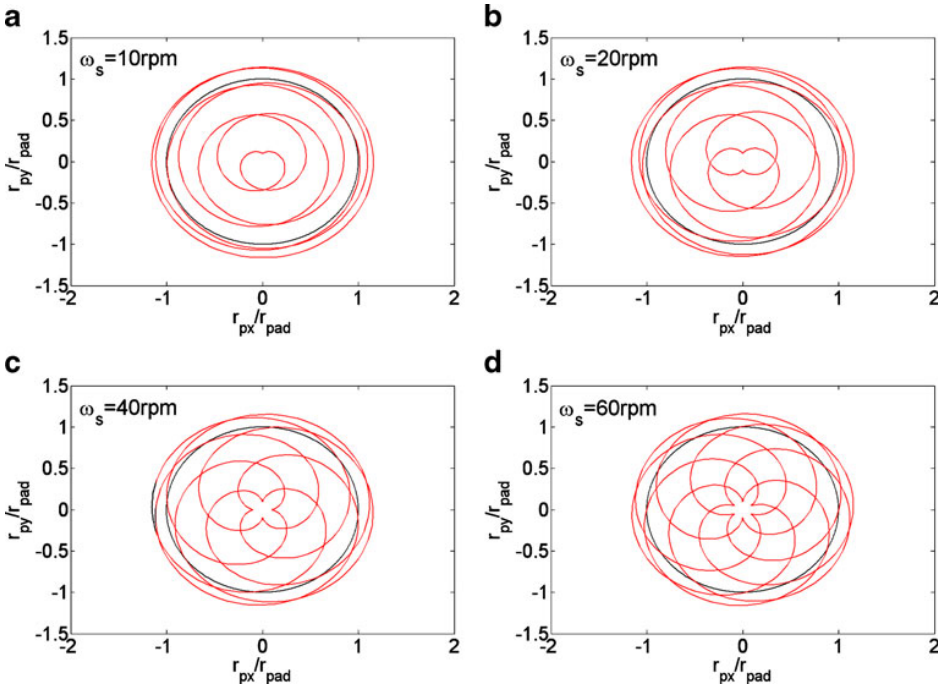

Fig. 6 Trajectories on the pad generated by one grain on the dresser center with different rotating speed ω_s. **a** ω_s=10 rpm, **b** ω_s=20 rpm, **c** ω_s=40 rpm, **d** ω_s=60 rpm (horizontal axis: r_{px}/r_{pad}, vertical axis: r_{py}/r_{pad})

implies the recovered areas and eventually the RARs are also different. Actually, at certain frequency ratios, the movements between the dresser and its associated pad become synchronous. As a result, the dresser can only cut pads at specific locations and the resulting RAR becomes extremely poor. A case study to demonstrate such an argument can be seen in Fig. 7. In both of these studies, most of the dressing parameters are the same (i.e., ω_p= 70 rpm, θ_i=90°, swing angle is between 0 and 40°, and the conditioning time is t=60 s). The only difference is the dressing speed ω_s (i.e., 50 versus 51 rpm). As one can see, the dresser with a 50 rpm rotating speed shows synchronization while the one with a 51 rpm results in a less synchronous motion; subsequently, a much higher RAR is obtained.

Next, the dressing capability of individual diamond grits is investigated since the trajectory on a pad for individual grits is different. Three different grit locations (r_d=560, 610, and 660 mm) are used in this study and their corresponding trajectories are shown in Fig. 8. In this study, the ω_R is fixed as 0.572, θ_i=180°, and t=6 s. It can be seen that these trajectories are different. As a result, in order to accurately determine the RAR, the trajectory of the dresser center may not be sufficient. Unfortunately, to the best of our knowledge, almost all related studies have focused on the trajectory of the dresser center only.

4.2 RAR demonstration

In order to perform parametric studies effectively, dimensionless parameters should be used instead of physical parameters. In this work, the dressing time and the rotating speed of the pad can be combined to form a normalized dressing time, t^*, which is defined as

$$t^* = t \times \omega_p. \tag{10}$$

Next, the RARs of flat and grooved (concentrated circled shape) pads at different t^* are studied and visualized. The

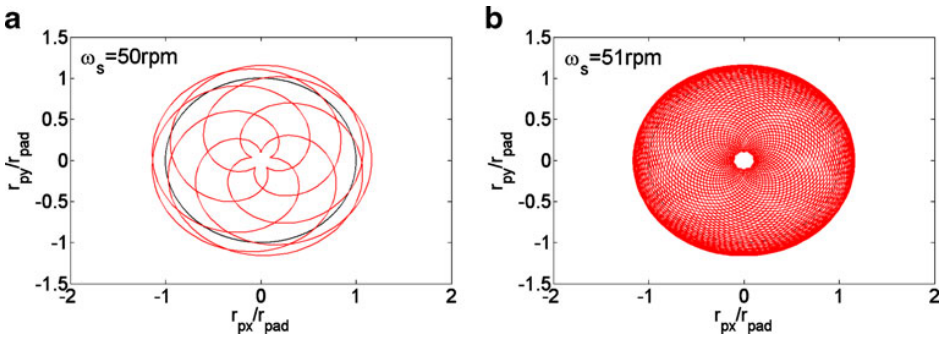

Fig. 7 Trajectories on the pad with different rotation ratio **a** ω_s=50 rpm, **b** ω_s=51 rpm (horizontal axis: r_{px}/r_{pad}, vertical axis: r_{py}/r_{pad})

SUNG EXHIBIT 2009
IPR2024-533

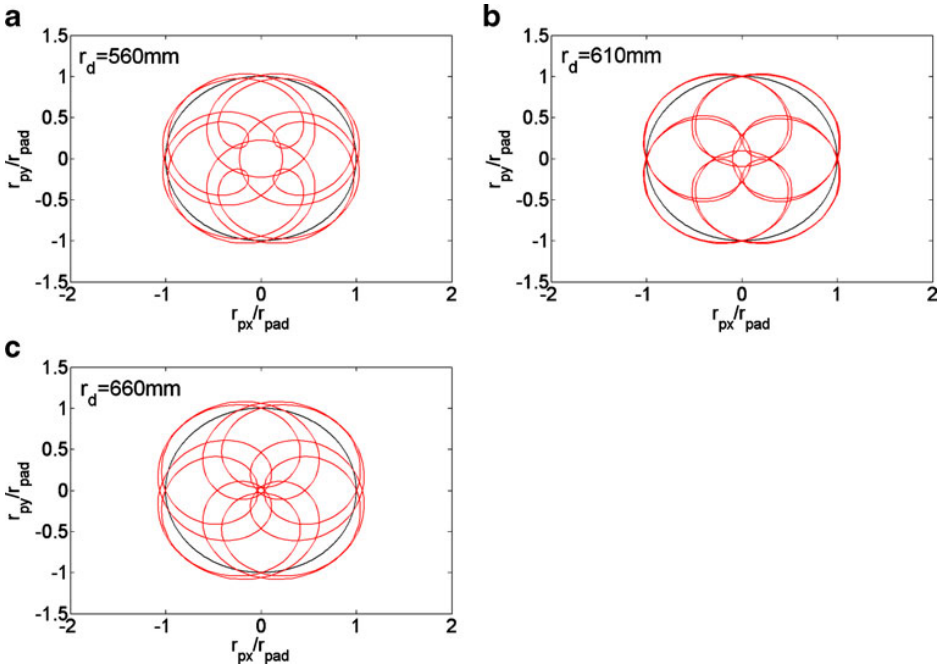

Fig. 8 Trajectories on the pad generated by one grain on the dresser with different r_d, **a** r_d=560 mm, **b** r_d=610 mm, **c** r_d=660 mm (horizontal axis: r_{px}/r_{pad}, vertical axis: r_{py}/r_{pad})

necessary parameter settings are listed in Table 2 and the dressing history between t^*=10 and 70 is shown in Fig. 9. Figure 9a shows the trajectory of the dresser center up to t^* equaling 70. The dressing depth contour of different t^* are then shown in Fig. 9b, d, and f. Finally, the dressing contours are then reduced to two colors (i.e., dark color, fully recovered areas; light color, not fully recovered portion). The effective cutting depth is 2 μm in this case [19], and the RARs are calculated and shown in Fig. 9c, e, and g. It can be seen that the portion of the fully recovered area increases with dressing time as one would expect. However, there are some specific pad locations that the dresser cannot meet and these locations remain undressed (or, strictly speaking, it takes much longer to finish the dressing) and the dressing parameters should be further optimized to reduce these undressed zones. Similar studies are then performed for a grooved pad using the same processing parameters and the results are shown in Fig. 10. The results are similar except that the grooves are shown in light color, since these areas are not used for polishing during a CMP process. Therefore, the only difference between these two cases concerns the effective contact area, and these results in a slightly higher contact pressure for the groove pads. As a result, the cutting depth for grooved pads is slightly higher than that for flat pads. Figure 11 shows a typical cutting profile for a typical cross section of pads. One can see that after t^* exceeds 70, the cutting depths for grooved pads are generally deeper than that of flat pads.

By changing the dressing parameters, the resulting RAR is also altered. One should be able to reach a reasonable RAR within a reasonable amount of dressing time. On the other hand, without careful consideration, it is also expected that the synchronization between the pad and dresser could result in a very poor RAR.

It is important to observe that the Preston's equation, as well as other CMP models, focuses on the influence of kinematics and stress and lumps all other effects into the Preston's constant. Physically, the decreased MRR during a CMP process due to the accumulation of debris and the recovery of the MRR by dressing suggest that there is a strong correlation between the Preston's constant and RAR.

Table 2 The parameter settings of flat and grooved pads

Dresser speed, ω_s (rpm)	40	Dresser radius, r_c (mm)	50
Pad speed, ω_p (rpm)	70	Pad radius, r_{pad} (mm)	390
Speed ratio, ω_R	0.572	Arm length, l (mm)	610
Dresser initial position, θ_i	90°	Grooved pitch (mm)	12
Dressing route	0–40°	Grooved depth (mm)	0.2
Dressing time, t^*	70	Grooved width (mm)	4

SUNG EXHIBIT 2009
IPR2024-533

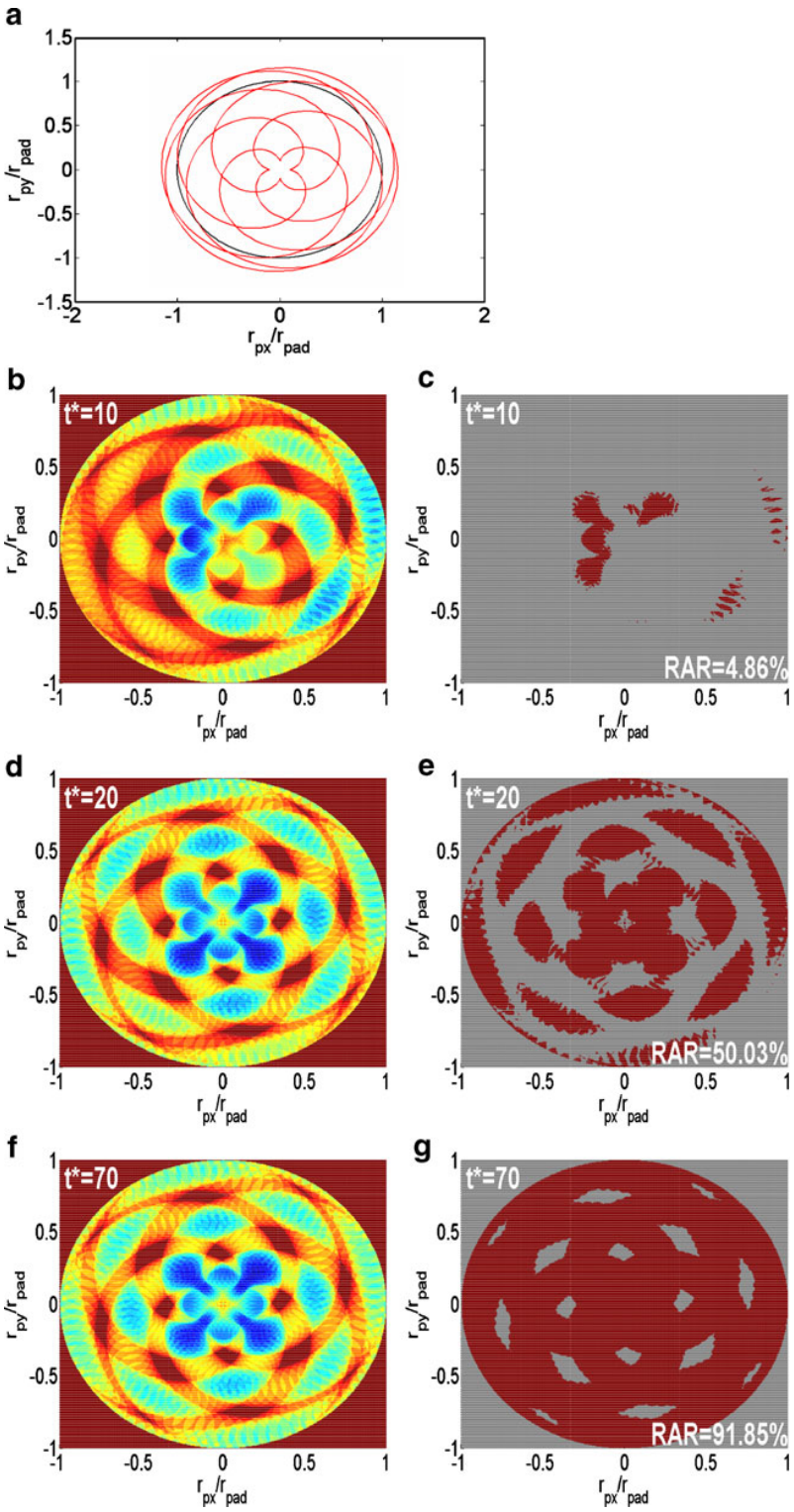

Fig. 9 The dressing contour and the resulted RARs of an ungrooved pad with different t^*, where $\omega_R=0.572$, $\theta_i=90°$, route=0–40°, **a** dressing trajectory, **b** the contour of pad at $t^*=10$, **c** RAR at $t^*=10$, **d** the contour of pad at $t^*=20$, **e** the RAR at $t^*=20$, **f** the contour of pad at $t^*=70$, **g** the RAR at $t^*=70$ (horizontal axis: r_{px}/r_{pad}, vertical axis r_{py}/r_{pad})

As a result, it is possible to postulate that the recovery extent of Preston's constant can be represented by the RAR. For example, a RAR of 90% implies that the Preston's constant is recovered by the same extent.

4.3 Parametric studies

After performing preliminary demonstrations, the effects of some key processing parameters for the pad dressing are

SUNG EXHIBIT 2009
IPR2024-533

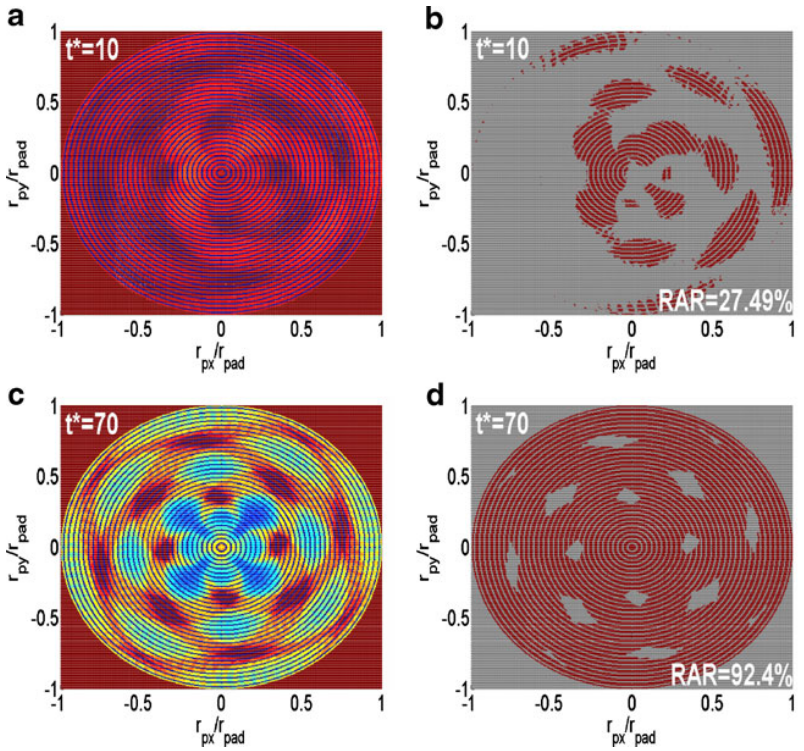

Fig. 10 The dressing contour and the resulted RARs of the grooved pad with different t^*, **a** the contour of pad at $t^*=10$, **b** RAR at $t^*=10$, **c** the contour of pad at $t^*=70$, **d** RAR at $t^*=70$ (horizontal axis: r_{px}/r_{pad}, vertical axis: r_{py}/r_{pad})

systematically investigated in this sub-section to understand their influences and to quantize their effects in terms of providing useful information for optimizing a dressing process. In this study, the operating parameters rather than the geometric parameters are chosen since there are no degrees of freedoms for process engineers to change in terms of the geometric settings for a commercialized dresser. Key operating parameters to be investigated in this section are speed ratio ω_R, dresser initial positions, and dressing routes.

4.3.1 The effect of dressing speed

In order to explore the effect of dressing speed, a pad rotating speed ω_P is fixed at 70 rpm, and changes to the dressing speed ω_S are limited such that the speed ratio ω_R varies between 0.143 and 1.144. In this study, the other parameters are fixed as: $\theta_i=90$; sweep angles 0–40°; $r_c=50$ mm, $r_{pad}=390$ mm. The relationships between t^* and the achieved RAR for different ω_R are shown in Fig. 12a. It is found that as t^* increases, the RARs are also increase as one would expect. Furthermore, when t^* is small, the RARs increase with ω_R since a larger ω_R implies a larger cutting area experienced within a given time. It is also interesting to point out that as ω_R approaches unity, its associated RAR initially rises quickly since the synchronization makes the cutting is so efficient during the first few rotations. However, as t^* increases further, the synchronization effect also causes a major portion of the pad to become useless for dressing, and the final RAR can only reach 25%. For a process engineer, one major concern is to achieve the best RAR within a reasonable time and to avoid the situation of synchronization. This issue can be seen in Fig. 12b. For example, if one only allows $t^*=30$, certainly, an $\omega_R=1.144$ is the best choice. However, if the target dressing time equals

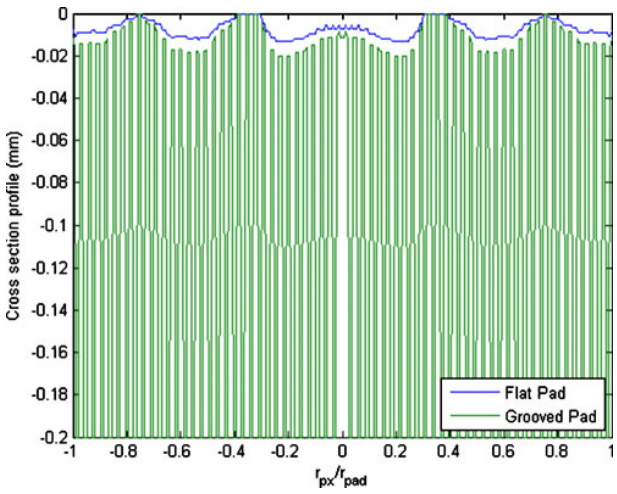

Fig. 11 The profile of ungrooved and grooved pads after t^* exceeds 70

SUNG EXHIBIT 2009
IPR2024-533

t^*=70, although ω_R=1.144 can still yield the best result, the difference with the other situations become less critical.

4.3.2 The effect of dresser initial position

The effect of the dresser's initial position is then investigated. Physically, as shown in Fig. 4, the difference in initial position can cause differences in both cutting speed and cover areas. In this parametric study, ω_R is fixed as 0.858 and the swept angle range is between 0 and 40°. r_{pad} and the distance between the pad and dresser centers are 390 and 38 mm, respectively. The initial positions chosen are θ_i=90° and 180°. Two dresser sizes with radii (r_c) equal to 30 and 50 mm are selected in this work. The achieved RARs with respect to t^* are shown in Fig. 13. It can be seen that the larger r_c (i.e., 50 mm) and θ_i of 180° yield a slightly larger RAR. On the other hand, the smaller r_c (i.e., 30 mm), the one with θ_i=90°, actually achieves a better RAR. This is because a small r_c with a route of θ_i=180° may not be able to cover the entire pad surface. However, as shown in Fig. 13, the differences are not significant.

4.3.3 The effect of dressing routes

The next parameter to be discussed is the influence of the dressing route. Two common routes, i.e., 0–40° and ±40° sinusoidal motions, are used. For a given dresser rotating speed, the ±40° can cover more pad area but requires a longer dressing time to finish one cycle. Such a trade off may need to be justified for a process design. Other fixed parameters in this study are ω_R=0.858, r_c=50 mm, r_{pad}= 390 mm, and θ_i=180°. The results are shown in Fig. 14. Both of the resulting RARs are saturated for t^* greater than 50. It can be seen that the RAR for the route of 0–40° is slightly greater than that of the route of ±40° since the former achieves a 95% RAR while the latter only achieves a 90% RAR.

4.3.4 The effect of dresser disk size

The size of the dresser disk is certainly an important parameter in terms of the dressing efficiency. Two situations are considered in this study. First, the back pressure is fixed and this implies the cutting depth for each time step is independent of the disk size. Second, if the total back load is fixed, the back pressure is reduced as r_c increases. In this situation, the cutting depth for each time step drops as r_c increases.

For the first situation, the simulation results are shown in Fig. 15a, where the fixed parameters are ω_R=0.143, r_{pad}= 390 mm, and θ_i=180°, while the dressing route is 0–40°. It can be found that for a given t^*, RAR increases with r_c as expected. However, if the applied load is fixed, the contact pressure decreases as the size of the dresser increases. Thus,

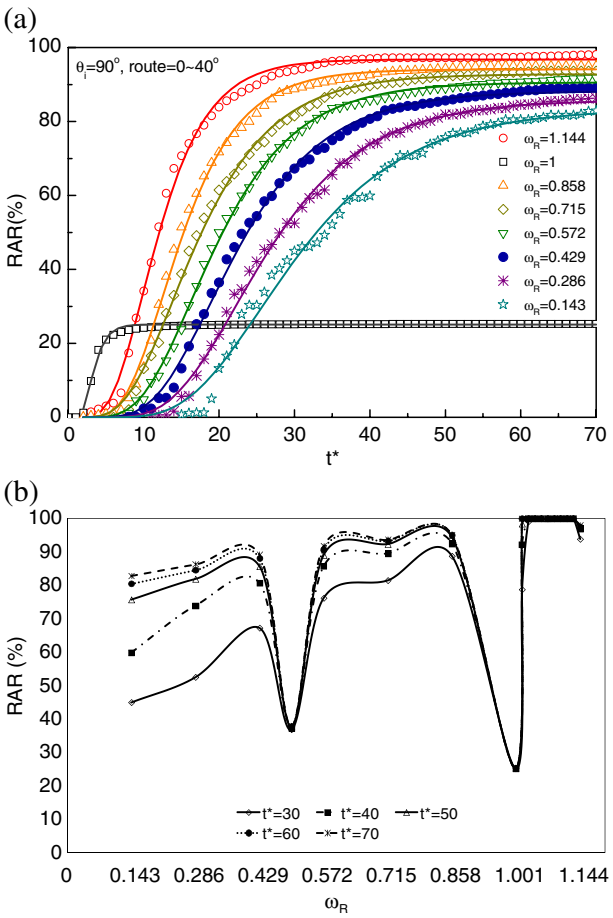

Fig. 12 The influence of ω_R on the resulted RAR, **a** the time histories with different ω_R, **b** the resulted RAR of various ω_R at different t^*

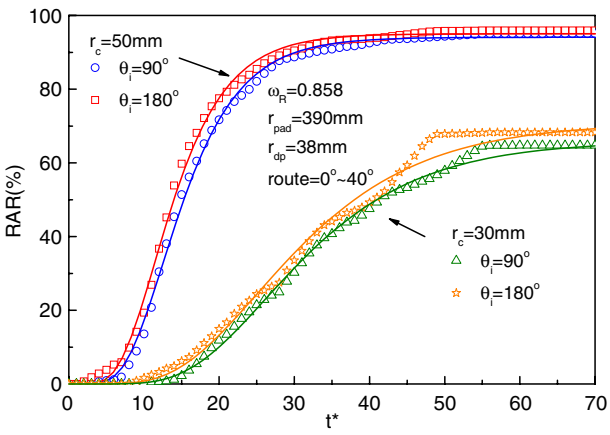

Fig. 13 The influence of the dresser initial position on the achieved RAR

SUNG EXHIBIT 2009
IPR2024-533

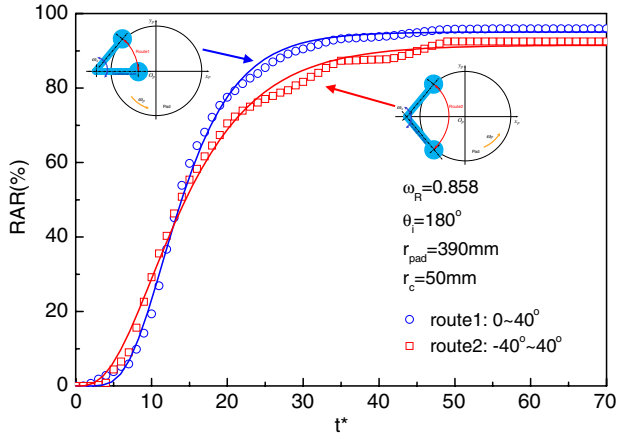

Fig. 14 The influence dressing routes on the resulted RAR

by Eq. 2, the dressing rate is reduced and more cutting is required to fully recover the pad. As a result, as shown in Fig. 15b, the increase in dresser size does not exhibit the obvious advantages of the first simulation situation. However, as shown in Fig. 15b, it is found that as t^* become longer, a dresser with a larger r_c generally yields a larger steady state RAR because that certain portion on the pad is possibly never dressed for use on a smaller dresser. A larger dresser can potentially eliminate these parts. On the other hand, it is also interesting to point out that during the initial cutting period (e.g., t^* less than 30 in Fig. 15b), the scenario is totally different for the steady state situation because a smaller dresser can perform at a higher dress rate and it may not need many revolutions to effectively recover the dressed area.

5 Discussion

This work develops a novel pad dressing emulator to evaluate the pad conditioning efficiency under different parameter settings. By proposing the new performance index, RAR, it is possible to quantify the influence of each key process or geometry parameter and to design efficient dressing schemes to reduce costs. In summary, the contributions of this work are addressed below.

First, unlike the previously proposed performance index CD, which only considers the cutting area, in this work, the proposed RAR can fully reflect the practical needs with better physical insights. Using RAR as the performance index, it is possible to perform more realistic parametric studies to quantify the influence of each dressing parameter.

Second, the emulator presented in this work should also be very useful for process engineers in terms of selecting appropriated processing parameters to optimize the pad conditioning process. Without using an emulator, the optimization of a dressing process relies entirely on a basis of experimental trial and error, which is costly. We believe that the presented pad conditioning emulator can effectively reduce the costs and shorten the time necessary to design the required processing parameters.

Finally, it is also important to re-state that the correlation between the performance index RAR and the overall recovery percentage of Preston's constant. That is, the dressing contour maps shown in Figs. 9 and 10 actually represent the distribution of Preston's constant, and the study links directly to the wafer level CMP simulation and emulation. To the best of our knowledge, this work is the first to address such a correlation.

In addition, from the parametric analyses addressed in Section 4, it is found that the most critical factor to influence the final resulting RAR is the rotating speed ratio ω_R. Usually, a larger ω_R results in a better RAR. However, if the rotating speeds of a pad and its associated dresser are synchronous, i.e., ω_R=1, 2, 3, and so on, the final RAR is poor. This situation should be avoided at every stage of the

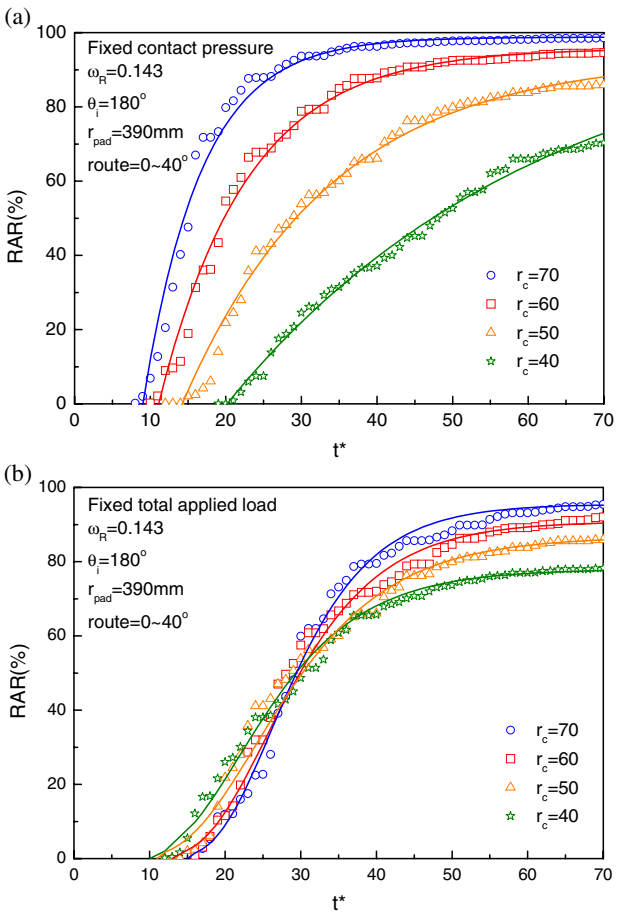

Fig. 15 The influence of dresser disk size on the resulted RAR, **a** the back pressure is fixed, **b** the total back load is fixed

SUNG EXHIBIT 2009
IPR2024-533

pad conditioning process. On the other hand, there are also some operational parameters such the initial positions and the dressing routes whose effects may not be important, and these effects may possibly be excluded from consideration during the process optimization.

Finally, as mentioned above, the dressing contour and RARs can be directly linked to the distribution and the averaged recovered Preston's constants. Through the effort of the pad conditioning emulator, the distribution information and the averaged recovered Preston's constant can be obtained. As a result, it is possible to integrate this pad conditioning module with our pre-developed wafer level CMP CAD emulator [20, 21], which is used to predict the contact stress and material removal rate, as well as the wafer profile during/after a CMP process, where Preston's constant plays a critical role in terms of obtaining accurate results. By such efforts, it is expected that the accuracy and reliability of wafer level CMP emulation can be further improved—we plan to devote ourselves to this research in the future.

6 Summary and conclusion

The chemical mechanical polishing process is a key fabrication route for the modern semiconductor process. The degradation of polishing pads during the polishing process can significantly influence the polishing performance. Therefore, pads need to be conditioned frequently. In this work, a pad condition simulation module is designed and demonstrated. In addition, a new performance index, the recover–area ratio, is defined. A series of parametric studies (such as speed ratio, sweeping angle range, initial position, and dresser size) are performed to investigate the influence of key geometric or processing parameters for a pad conditioning process to optimize the conditioning performance. It is found that the speed ratio ω_R plays the most critical role in terms of influencing dressing performance. Finally, it is possible to correlate the pad RAR and Preston's constant variation and to integrate the pad conditioning emulator with the pre-developed CMP polishing simulation module as a whole utility to further optimize the existing CMP process.

Acknowledgments This work is supported by National Science Council (NSC) of Taiwan under the contract number NSC-95-2221-E-006-399-MY2 and Taiwan Semiconductor Manufacturing Company (TSMC) under contract numbers 95S003 and 96S073 with Drs. S-M Cheng and Y-W Chou as the technical monitors. The invaluable discussion and comments from Prof. T-S Yang at NCKU and Dr. T-C Tseng formerly at TSMC are greatly appreciated.

Reference

1. Zantye PB, Kumar A, Sikder AK (2004) Chemical mechanical planarization for microelectronics applications. Mater Sci Eng R 45:89–220
2. Preston F (1927) Optimization of computer controlled polishing. Glass Tech 11:214–219
3. Zhou C, Shan L, Hight JR, Ng SH, Danyluk S (2002) Fluid pressure and its effects on chemical mechanical polishing. Wear 253(3–4):430–437
4. Wang YC, Yang TS (2007) Effects of pad grooves on chemical mechanical planarization. J Electrochem Soc 154(6):H486–H494
5. Hooper BJ, Byrne G, Galligan S (2002) Pad conditioning in chemical mechanical polishing. J Mater Process Technol 123:107–113
6. McGrath J, Davis C (2004) Polishing pad surface characterisation in chemical mechanical planarization. J Mater Process Technol 153–154:666–673
7. Park KH, Kim HJ, Chang OM, Jeong HD (2007) Effects of pad properties on material removal in chemical mechanical polishing. J Mater Process Technol 187–188:73–76
8. Lin YY, Lo SP (2003) A study on the stress and nonuniformity of the wafer surface for the chemical-mechanical polishing process. Int J Adv Manuf Technol 22:401–409
9. Lin YY, Lo SP (2004) A study of a finite element model for the chemical mechanical polishing process. Int J Adv Manuf Technol 23:644–650
10. Chiu JT, Lin YY (2008) Modal analysis of multi-layer structure for chemical mechanical polishing process. Int J Adv Manuf Technol 37:83–91
11. Lo SP, Lin YY, Huang JC (2007) Analysis of retaining ring using finite element simulation in chemical mechanical polishing process. Int J Adv Manuf Technol 34:547–555
12. Liao YS, Hong PW, Yang CT (2004) A study of the characteristics of the diamond dresser in the CMP process. Key Engineering Materials 257–258:371–376
13. Zhou ZZ, Yuan JL, Lv BH, Zheng JJ (2008) Study on pad conditioning parameters in silicon wafer CMP process. Key Engineering Materials 359–360:309–313
14. Sung J, Pai YL (2000) CMP pad dresser: A diamond grid solution. In Advances in Abrasive Technology III 189–196, Soc. Grinding Engineers
15. Tso PL, Ho SY (2007) Factors influencing the dressing rate of chemical mechanical polishing pad conditioning. Int J Adv Manuf Technol 33:720–724
16. Tso PL, Hsu R (2007) Estimating chemical mechanical polishing pad wear with compressibility. Int J Adv Manuf Technol 32:682–689
17. Hu CC (2004) Modeling of chemical mechanical polishing. M.S. thesis, Dept. Mech. Eng., DEKALB ILLINOIS, USA
18. Tyan F (2007) Pad conditioning density distribution in CMP process with diamond dresser. IEEE Trans Semicond Manuf 20(4):464–475
19. Liao YM, Yan HY, Wang FJ, Chen KS (2006) Mechanical properties characterization for CMP pads. 23rd National Conference of the Chinese Society of Mechanical Engineers, Tainan, Taiwan
20. Chen KS, Yeh HM, Yan JL, Chen YT (2009) Finite-element analysis on wafer-level CMP contact stress: reinvestigated issues and the effects of selected process parameters. Int J Adv Manuf Technol 42:1118–1130
21. Yeh HM (2009) Development and applications of process emulators for MEMS and semiconductor fabrication processing. Ph.D. dissertation, Dept. Mech. Eng., National Cheng-Kung University, Tainan, Taiwan

SUNG EXHIBIT 2009
IPR2024-533